

Traces of a triboson resonance

J. A. Aguilar-Saavedra^a, J. H. Collins^{b,c,d}, S. Lombardo^d

^a Departamento de Física Teórica y del Cosmos, Universidad de Granada,

E-18071 Granada, Spain

^b Maryland Center for Fundamental Physics, University of Maryland, College Park, MD 20742

^c Department of Physics and Astronomy, Johns Hopkins University, Baltimore,

MD 21218, USA

^d Department of Physics, LEPP, Cornell University, Ithaca, NY 14853, USA

Abstract

We show that the relatively small but coincident excesses observed around 2 TeV in the ATLAS Run 1 and Run 2 hadronic diboson searches — when a cut on the number of tracks in the fat jets is not applied — and the null results of all remaining high-mass diboson searches are compatible with the decay of a triboson resonance R into WZ plus an extra particle X . These decays can take place via new neutral (Y^0) or charged (Y^\pm) particles, namely $R \rightarrow Y^0 W$, with $Y^0 \rightarrow ZX$, or $R \rightarrow Y^\pm Z$, with $Y^\pm \rightarrow WX$. An obvious candidate for such intermediate particle is a neutral one Y^0 , given a 3.9σ excess found at 650 GeV by the CMS Collaboration in searches for intermediate mass diboson resonances decaying to ZV , with $V = W, Z$. We discuss discovery strategies for triboson resonances with small modifications of existing hadronic searches.

1 Introduction

New physics may show up in the searches performed at the Large Hadron Collider (LHC) in unexpected ways. The ATLAS and CMS experiments perform a large number of measurements in a variety of final states targetting simple “benchmark” novel signatures but, if a sign of new physics beyond the Standard Model (SM) eventually appears, its real source may well be different from the specific signature searched. In the LHC Run 1 at a centre-of-mass (CM) energy of 8 TeV the most remarkable deviation from the SM prediction was a 3.4σ excess found by the ATLAS Collaboration [1] in the search for heavy resonances decaying into two SM gauge bosons $V = W/Z$ — also known as a diboson resonances — with the bosons decaying hadronically, giving rise to two fat jets J . The excess was compatible with a new heavy resonance with a mass around 2 TeV, and it was largest in the WZ channel where the two bosons were respectively tagged as a W and a Z boson. An analogous search performed by the CMS Collaboration [2] also found

an excess at the 2σ level around this mass. But searches performed in the semileptonic decay modes of the WZ diboson pair [3–5], some of them more sensitive than the hadronic mode, showed no hint of an excess at this mass.

The absence of any other signals motivated the proposal [6] that the anomaly might be due to a triboson resonance, namely, a heavy resonance R with a mass around 2 TeV decaying into one gauge boson plus an intermediate neutral or charged particle, $R \rightarrow Y^0 W$ or $R \rightarrow Y^\pm Z$, or perhaps both, where the masses of the intermediate particles Y^0, Y^\pm could in principle lie in a wide range 300 – 1000 GeV. The subsequent decays of Y^0 and Y^\pm into a gauge boson plus some extra particle X , $Y^0 \rightarrow ZX$ and $Y^\pm \rightarrow WX$, would produce a WZX triboson signal. And, for this signal, the presence of the extra particle X , which could be the SM Higgs boson H , a W/Z boson or a new particle with a mass $M_X \lesssim 300$ GeV, would make the searches in the semileptonic channels much less sensitive than for a diboson resonance $R \rightarrow WZ$. Such a WZX signal could be realised, for example, in left-right (LR) models when $\tan\beta \equiv v_2/v_1$, that is, the ratio of the vacuum expectation values (VEVs) of the two scalars ϕ_1, ϕ_2 in the bidoublet, is either very small or very large [7], that is, one of the VEVs is much larger than the other. In that case, the W' boson plays the role of the heavy resonance R and the decays $W' \rightarrow WZ$, with a rate proportional to $\sin^2 2\beta$, are absent. But the decays into heavy scalars, e.g. $W' \rightarrow WH_1^0$, $W' \rightarrow H^\pm Z$, with a rate proportional to $\cos^2 2\beta$, are allowed. The subsequent cascade decay of the heavy scalars $H_1^0 \rightarrow ZA^0$, $H^\pm \rightarrow WA^0$, with A^0 a lighter pseudo-scalar, or $H_1^0 \rightarrow ZH$, $H^\pm \rightarrow WH$, yield triboson signals.

At the LHC Run 2, with a CM energy of 13 TeV, searches for diboson resonances have been performed using data taken in 2015. Searches in the semileptonic channels [8–11] have not shown any deviation from the SM prediction at this mass and searches in the hadronic channel [11, 12] have not confirmed the previously seen excess. Still, the data are not conclusive enough, and the examination of experimental results in the context of triboson signals is worthwhile. This is the main purpose of this paper. In section 2 we discuss in detail the measurements performed by the ATLAS Collaboration in their searches for diboson resonances decaying hadronically, with their similarities and differences. In section 3 we present our detailed Monte Carlo calculations of the QCD dijet background, which do not show any trace of a bump caused by the jet tagging criteria. Section 4 is devoted to present predictions for several selected benchmark scenarios of triboson resonances in a variety of diboson searches. In this respect, the appearance of a 3.9σ excess in a CMS search for low-mass diboson resonances [13] decaying into two opposite-sign leptons and a boson-tagged jet ($\ell\ell J$), at a mass of 650 GeV, indicates that the cascade decays of the heavy resonance can be mediated by a neutral particle Y^0 with this mass. In section 5 we propose discovery strategies for triboson resonances in the

fully hadronic ATLAS search, with minimal changes with respect to the analysis currently carried out. In section 6 we discuss our results and their implications on the heavy neutral gauge boson that should accompany the charged resonance presumably responsible for a WZX signal.

2 Closer look at fat dijet measurements

As aforementioned, the ATLAS Collaboration found a 3.4σ excess in Run 1 data at 8 TeV with a luminosity of 20.3 fb^{-1} . For the reader's convenience, we reproduce in figure 1 (left) the number of events with the nominal WZ ATLAS selection, with the background-only best fit. With Run 2 data at 13 TeV, the ATLAS Collaboration performed a search using 3.2 fb^{-1} . Given the similar efficiencies of both searches and the $7-8$ times larger $q\bar{q}$ partonic luminosity at 13 TeV, which compensates the smaller luminosity, a similar excess of around 8 events at 2 TeV was expected in Run 2, but the data, shown in figure 1 (right) show no significant deviation and are compatible with the background-only hypothesis at the 1σ level.

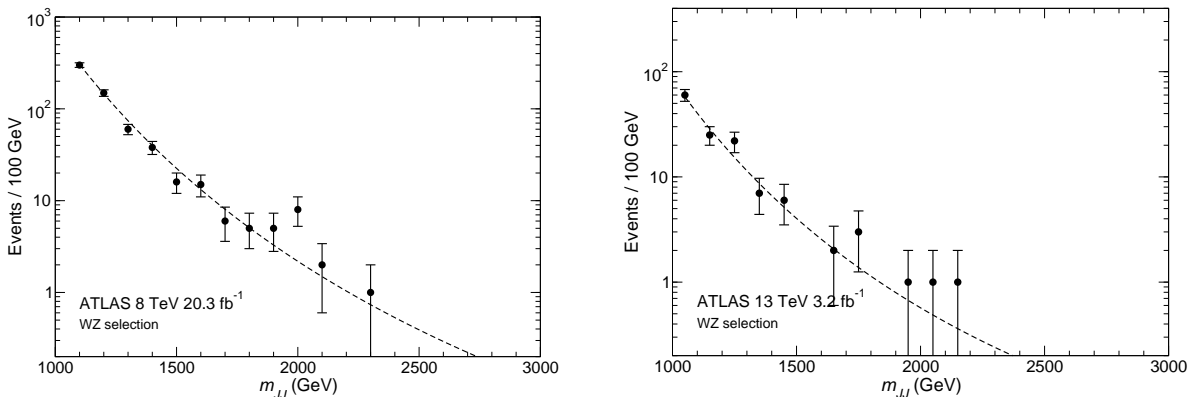


Figure 1: Number of events with the nominal ATLAS WZ selection in Run 1 (left) and Run 2 (right). The dashed lines correspond to the background-only fit.

Besides data with the nominal selection, the ATLAS Collaboration has released results when one of the V boson jet tagging requirements is dropped. We recall here that in the Run 1 analysis fat jets are reconstructed with the Cambridge-Aachen algorithm [14] with radius $R = 1.2$, while in the Run 2 analysis the jets are reconstructed with the anti- k_T algorithm [15] with $R = 1.0$. Several requirements are made on the reconstructed fat jets to be tagged as W or Z jets (for further details see [1, 12]).

- A cut $\sqrt{y} \geq 0.45$ on the y variable [16] measuring the subjet momentum balance,

which is replaced by a cut on the so-called D_2 function [17] in Run 2. The precise value of the cut on D_2 depends on the jet transverse momentum.

- A cut on the jet mass: $|m_J - M_V| < 13$ GeV, with $M_V = 82.4$ GeV (92.8 GeV) for W (Z) bosons in Run 1. The cut is $|m_J - M_V| < 15$ GeV, with $M_V = 83.2$ GeV (93.4 GeV) in Run 2.
- A requirement on the number of tracks with transverse momentum $p_T > 0.5$ GeV and originating from the primary vertex, $N_{\text{trk}} < 30$.

Interestingly enough, Run 2 data when one of these three jet tagging requirements is removed also display bumps around 2 TeV, as it has already been pointed out [7]. We will focus on results without the N_{trk} cut, as the corresponding numbers of data events are the closest to the ones with the nominal selection (in other words, removal of this requirement yields a smaller decrease of the expected signal significance than either the removal of the jet mass or the removal of the \sqrt{y}/D_2 cuts). We give in figure 2 the number of events in the Run 1 [18] and Run 2 [12] analyses for the WZ selection without N_{trk} . The dashed lines are the background-only best-fit, calculated with a maximum likelihood fit using the same background parameterisation of the ATLAS Collaboration. For illustration we also include simple signal plus background fits using for the signal a Gaussian with centre 1950 GeV (1900 GeV) for Run 1 (Run 2) and a width of 70 GeV in both cases. The estimated statistical significance of the bumps in the data, evaluated from the likelihood, is 2.5σ at Run 1 and 2.4σ at Run 2. The approximate size of the excesses found from the signal plus background fit to data is quite compatible: 13 events in Run 1 and 10 events in Run 2.

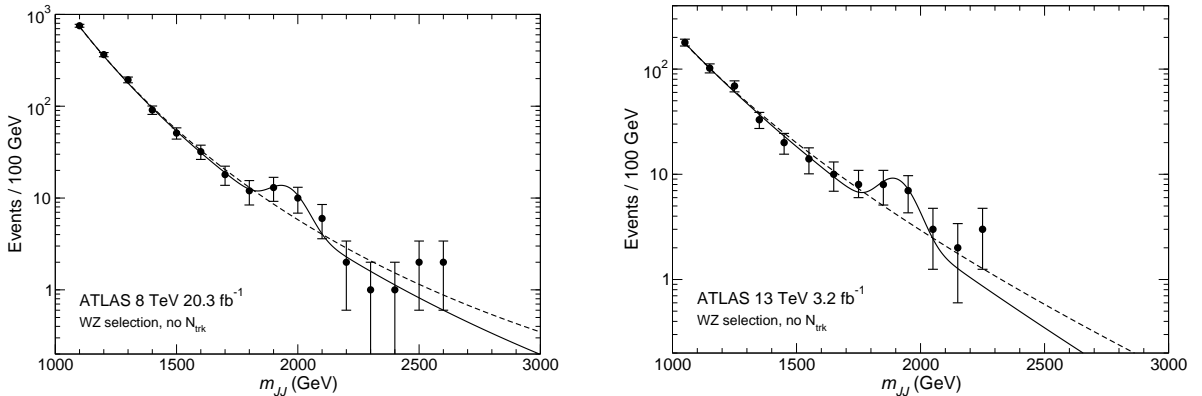


Figure 2: Number of events with the nominal ATLAS WZ selection except the N_{trk} cut in Run 1 (left) and Run 2 (right). The dashed lines correspond to the background-only fit. The solid lines show a simple signal plus background fit (see the text).

At this point, the urging question arises of why, if the data with the WZ selection without the N_{trk} cut show a consistent (but still not statistically significant) excess in both analyses, the results with the nominal selection (including the N_{trk} cut) are somewhat different. Let us discuss different possibilities in turn.

Statistics only. The coincidence of the the bumps at 8 and 13 TeV, plus some other excesses around 2 TeV like the CMS excess in $eejj$ production [19], disfavour the hypothesis that all these bumps are statistical fluctuations in data. Still, this is an open possibility given the relatively small significance of the bumps. In any case, new data will elucidate whether these excesses are merely statistical artifacts or not.

Mismodeling effects. It has been pointed out [20] that the jet tagging requirements may cause a slope change in the continuum QCD dijet distribution. However, as it can be seen by eye in figure 2, the observed bumps do not seem to be a slope change. As we will see in section 3, there is a slight change of slope in the Monte Carlo prediction for the QCD background. This change may affect the apparent size of a possible signal but does not give rise to a bump in the distributions. Besides, if the excess events at the bumps correspond to the very same QCD background as at the side bands, it is hard to conceive why in Run 1 data the further application of the N_{trk} cut shapes a peak, whereas in Run 2 data the N_{trk} cut flattens the bump.

New physics. The efficiencies of the N_{trk} cut have been evaluated by the ATLAS Collaboration using diboson signals and will generally be different for a different signal, *e.g.* a triboson. In order to explain the cleaning up of the bump in Run 2 data without resort to large statistical fluctuations, a new physics signal would be required for which (i) the combination of cuts on jet mass, D_2 and N_{trk} for $R = 1.0$ jets in Run 2 severely decreases the efficiency; (ii) but the combination of cuts on jet mass, \sqrt{y} and N_{trk} for $R = 1.2$ jets in Run 1 does not. In this regard, we have explored in appendix B several WZX triboson signals in several phase space regions and have found that, after the application of the remaining boson tagging cuts, the effect of the N_{trk} cut is very similar for the Run 1 and Run 2 analyses.

New physics and statistical fluctuations. On the other hand, given the small statistics of the samples with the nominal WZ selection, it might be possible that there is a downward fluctuation in Run 2 data and perhaps an upward fluctuation un Run 1 data. This possibility will, again, be tested when more data are available.

New physics and mismodeling effects. It is also possible that for new physics different from diboson resonances, the jet tagging variables are not correctly modeled by Monte Carlo simulations. Here it is worth pointing out that N_{trk} is not well modeled by simulation [21]. In the Run 1 analysis the ATLAS Collaboration derives a scale factor of 0.9 to

correct the efficiency of the N_{trk} cut for W and Z bosons given by the simulation, while in the Run 2 analysis the number of tracks given by the simulation is multiplied by 1.07. Despite these corrections being of the order of 10%, it is conceivable that for fat jets from the multiboson cascade decay of a TeV-scale particle the agreement between simulation and data is worse, maybe with some unknown correlation between N_{trk} and other tagging variables. We also point out that the CMS Collaboration has chosen not to use N_{trk} to improve the expected signal significance, neither in the Run 1 nor in the Run 2 searches.

From the above discussion, we can conclude that the most likely explanations of the found excesses, if they persist with more data and become statistically significant, are (i) a new physics signal, for example a triboson, but also with some Monte Carlo mismodeling effect in jet substructure variables, perhaps in N_{trk} ; (ii) some new physics signal far more complex than a triboson, in which case one would have also to justify why the excesses seen in the ATLAS searches are localised.

3 The QCD dijet background

In order to obtain a prediction for the QCD background, we fully recast Run 1 and Run 2 hadronic diboson searches from the ATLAS Collaboration [1, 12]. The full details of our procedure are given in appendix A. We generate dijet events at 8 and 13 TeV with MADGRAPH5 [22], dividing the phase space in slices of 100 GeV of dijet invariant mass, from 700 GeV to 4 TeV. Event generation is followed by hadronisation and parton showering with PYTHIA 8 [23]. Detector response is simulated with DELPHES 3 [24], and FASTJET [25] is used to perform jet physics. For each slice of dijet invariant mass, 5×10^5 events are simulated, and the results of each slice are weighed by the corresponding cross section and recombined to get the final (unnormalised) invariant mass distributions. Finally, a common scale factor is applied to all distributions — and different for 8 and 13 TeV —, so that the distributions without boson tagging are, to a good approximation, normalised to the measured ones for 20.3 fb^{-1} in Run 1 and 3.2 fb^{-1} in Run 2.

Our results are presented in figure 3. For Run 1, a slope decrease is visible around 1.7 TeV in the distributions with full WZ tagging (black) and without N_{trk} (pink). (In the distribution without \sqrt{y} there is a slope change too around 1.8 TeV.) The appearance of these “knees” may cause that the apparent size of an excess near 2 TeV is two or three events larger than the actual size of the excess, and the extracted significance is consequently overestimated. For Run 2 there is also a slope decrease but milder and near 1.5 – 1.6 TeV. The effect of the slope change on the significance of a bump at 2 TeV is expected to be much milder and likely absorbed in the fit.

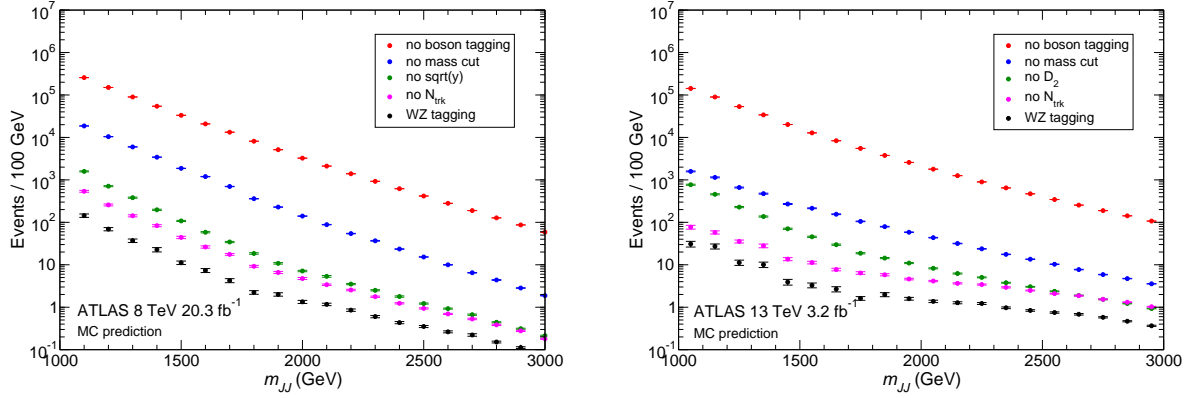


Figure 3: Monte Carlo predictions for the QCD dijet background, in Run 1 (left) and Run 2 (right). The error bars in the points represent the Monte Carlo uncertainty.

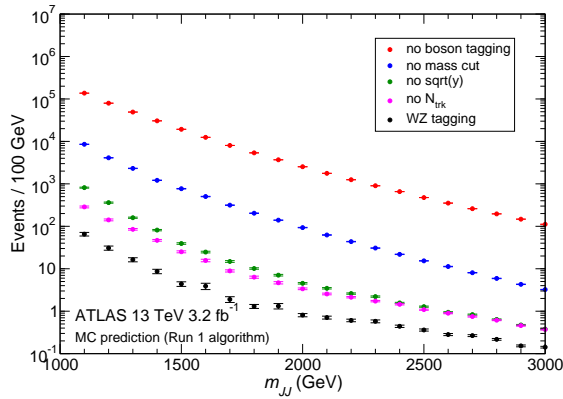


Figure 4: Monte Carlo predictions for the QCD dijet background in Run 2, using the Run 1 analysis. The error bars in the points represent the Monte Carlo uncertainty.

It is also interesting to look at the background prediction for Run 2 but using the jet reconstruction and tagging of the Run 1 analysis. This is presented in figure 4. We can observe that the change of slope near 1.7 TeV is similar to the one observed for the Run 1 analysis, namely figure 3 (left). Therefore, apparently the differences between the “knees” observed in our dijet simulations for Run 1 and Run 2 are caused by the jet reconstruction and tagging, rather than the CM energy.

4 Triboson signals in diboson searches

In this section we explore benchmark triboson resonance scenarios and their potential signals in several final states. With this purpose, we fully recast several ATLAS and CMS diboson searches. The signals are generated at parton level with PROTOS [26], using benchmark scenarios with $M_{W'} = 2.25$ TeV, $M_Y = 650$ GeV, and (i) $X = H$; (ii) $X = A$, a light pseudo-scalar particle with mass $M_A \simeq M_Z$ and decays $A \rightarrow b\bar{b}$; (iii) $X = A$, with decays $A \rightarrow q\bar{q}$. For Y^0 the choice of the mass is obvious from the CMS excess [13] and for Y^\pm we take the same value for simplicity, despite the fact that their masses do not need to be the same [7]. A heavier X is also allowed, but if its mass is much larger than M_Z the decays $Y^0 \rightarrow ZX$ cannot explain the CMS excess. For each benchmark and CM energy a sample of 5×10^4 events is generated and passed through showering and detector simulation with different DELPHES cards with settings adequate according to the experimental analysis considered. Additional details of our simulations are given in appendix A.

4.1 ATLAS searches in the fully hadronic channel

We begin with the Run 2 analysis focusing on the WZ selection without the N_{trk} cut, and use the excess of events over the background only expectation in the analysis of Ref. [12] to fix the overall normalisation of our potential signals in all channels. Specifically, we require 10 signal events in the invariant mass interval 1.7 – 2.1 TeV. The m_{JJ} distributions with this normalisation for the two possible W' cascade decay channels, $W' \rightarrow WY^0 \rightarrow WZX$, $W' \rightarrow ZY^\pm \rightarrow WZX$, are presented in figure 5 (top). In all cases, the distributions have a peaked shape, in agreement with the earlier results [6] obtained with a much less elaborate simulation. We point out that the peaked shape of the dijet invariant mass distribution for triboson signals in the ATLAS analyses is rather independent of the mass of the intermediate particle, and results are quite similar in this respect for masses from 300 GeV to 1 TeV. The efficiencies found for these channels is collected in table 1, for neutral (Y^0) and charged (Y^\pm) intermediate particles. These efficiencies are comparable to the efficiency of 0.09 found for a WZ diboson signal without N_{trk} . The efficiency penalty of $1/3 - 2/3$ for triboson signals is much smaller than the value of $1/7$ estimated in Ref. [6] with a more simplistic analysis, because kinematical configurations where two of the bosons merge into a single jet, that were discarded there, may also pass the event selection criteria due to the filtering performed on the jets. As a consequence, the coupling of the W' boson eventually required to explain the size of the excess is not too large and remains perturbative (see section 6).

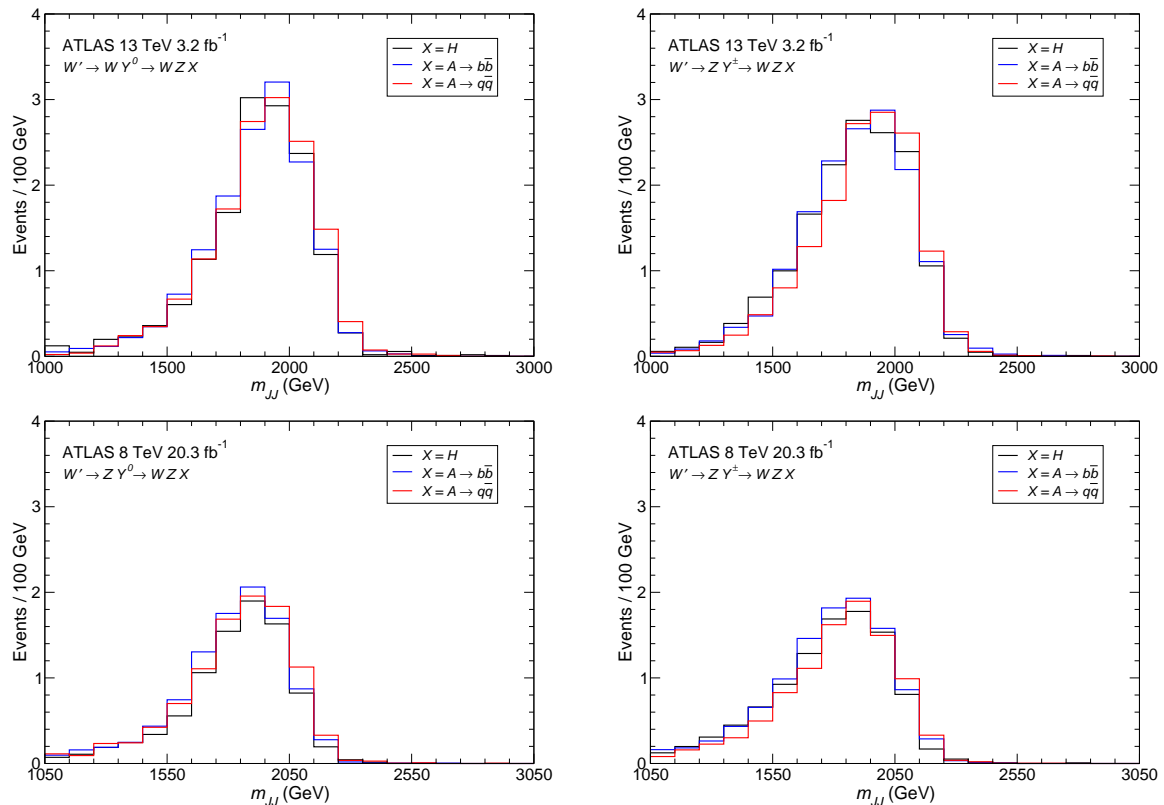


Figure 5: Top: Dijet invariant mass distribution for triboson signals in the ATLAS Run 2 fully hadronic analysis [12], in the WZ selection without N_{trk} . Bottom: the same, for the Run 1 analysis [1].

	$X = H$	$X = A \rightarrow b\bar{b}$	$X = A \rightarrow q\bar{q}$
Y^0	0.030	0.050	0.055
Y^\pm	0.032	0.058	0.066

Table 1: Efficiencies for triboson signals, relative to the full WZX samples with all possible decays, for the ATLAS Run 2 fully hadronic analysis [12], in the WZ selection without N_{trk} .

For the Run 1 ATLAS analysis with 20.3 fb^{-1} we obtain the distributions in figure 5 (bottom) for the WZ selection without the N_{trk} cut. The same signal normalisations are used, with a scaling factor of $1/8.3$ for the cross section for 8 TeV respect to 13 TeV (with $M_{W'} = 2.25 \text{ TeV}$), and the corresponding luminosity scaling. The predicted size of the signals is smaller than in the Run 2 analysis, 3–4 events fewer at the 1.7–2.1 TeV invariant mass interval, due to two effects: first, the efficiencies, collected in table 2, are slightly smaller; second, for a W' mass of 2.25 TeV the larger luminosity does not compensate

the smaller cross section at 8 TeV. As we have seen in section 2, the fitted excess in Run 1 is larger than in Run 2; however, as argued in section 3, a knee in the background distribution could cause an apparent excess of a few events as well. Furthermore, in a sample of around 10 events one also expects statistical fluctuations to have some relevance.

	$X = H$	$X = A \rightarrow b\bar{b}$	$X = A \rightarrow q\bar{q}$
Y^0	0.025	0.046	0.051
Y^\pm	0.028	0.054	0.059

Table 2: Efficiencies for triboson signals, relative to the full WZX samples with all possible decays, for the ATLAS Run 1 fully hadronic analysis [1], in the WZ selection without N_{trk} .

4.2 CMS searches in the fully hadronic channel

The search for diboson resonances decaying into two fat jets performed by the CMS Collaboration with 8 TeV data and a luminosity of 19.7 fb^{-1} [2] showed a small excess, near the 2σ level, in the $1.5 - 2$ TeV range, whereas the search at 13 TeV with 2.6 fb^{-1} , with a similar sensitivity for 2 TeV resonances, is compatible with the SM expectation at the 1σ level. We give our results for the CMS Run 1 analysis in figure 6 (top), considering the high-purity sample. (The signal efficiency for the low-purity sample is similar and the background much larger.) In this analysis, the discrimination between W and Z bosons is not attempted, and jet masses in the interval $70 - 100$ GeV are considered. We use the same signal normalisations as before, and with a scale factor of $1/8.3$ for 8 TeV cross sections. In contrast to the ATLAS searches, here the dijet invariant mass distributions of the triboson signals are wider, in the $1.5 - 2$ TeV range, with around one event per 100 GeV. These predictions are quite compatible with the measurements.

In the Run 2 search the CMS Collaboration follows a slightly different strategy and divides the boson-tagged dijet samples into WW , WZ and ZZ , where a jet is considered as W -tagged if its mass is in the range $65 - 85$ GeV, and Z -tagged for a mass in the range $85 - 105$ GeV. We give in figure 6 (bottom) the predictions for the high-purity WZ -tagged sample, which amount to less than one signal event per 100 GeV. These predictions are also compatible with the measurements, where a handful of extra events above the SM prediction, as well as some downward fluctuations, are seen over the $1.5 - 2$ TeV range in the different WW , WZ and ZZ samples.

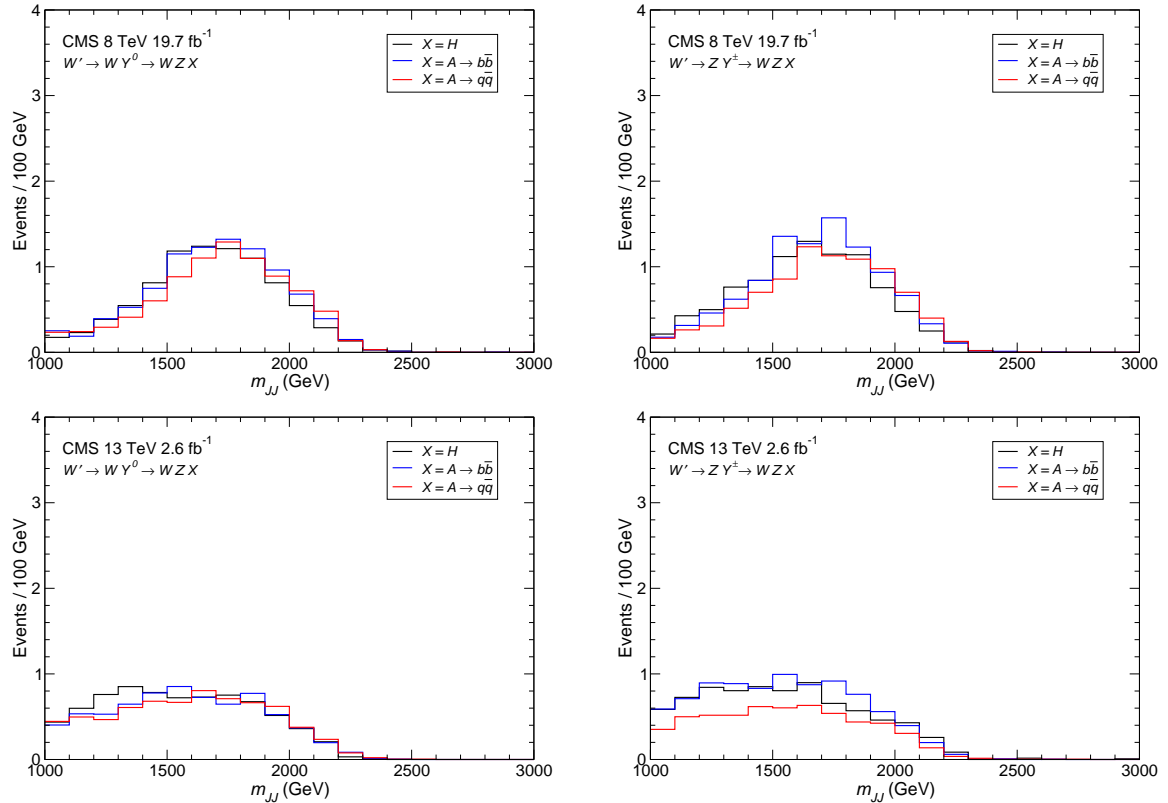


Figure 6: Dijet invariant mass distribution for triboson signals in the CMS Run 1 [2] (top) and Run 2 [11] (bottom) fully hadronic analyses, in the high-purity sample.

4.3 ATLAS Run 2 search in the $\nu\nu J$ channel

The $\nu\nu J$ channel (i.e. a final state with a single fat jet plus large missing energy) provides the best sensitivity to diboson resonances among the searches performed by the ATLAS Collaboration with Run 2 data [10]. In this search, the diboson mass cannot be directly reconstructed and, instead, the event transverse mass m_T is considered. It turns out that the sensitivity of this channel to triboson resonances is very poor, since the event selection requires the missing transverse energy vector to be isolated from any other jets (which is infrequent in the case of a triboson resonance) and also vetoes any charged lepton, often present in the final state under consideration. For these reasons, the sensitivity to triboson resonances is a factor 10 – 15 worse than in the fully hadronic channel. We present our results for this analysis in figure 7, with the same signal normalisation used in previous examples. The expectation for a signal that reproduces the ATLAS Run 2 dijet excess is one or at most two events in the 1.5 – 2 TeV range, perfectly compatible with the null results of this search.

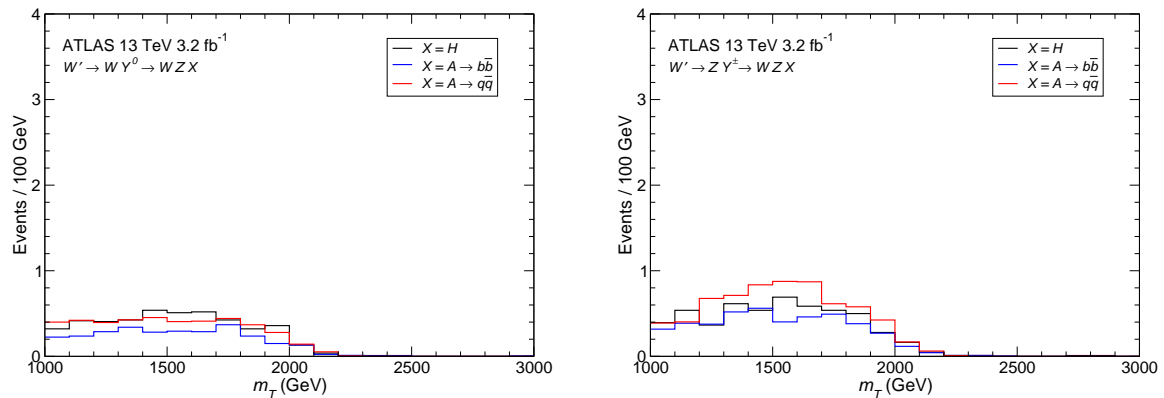


Figure 7: Transverse mass distribution for triboson signals in the ATLAS Run 2 $\nu\nu J$ analysis [10], in the WZ selection.

4.4 ATLAS Run 2 search in the $\ell\nu J$ channel

This channel [8, 11], in which the final state has a charged lepton ℓ , large missing energy and a fat jet, is also very sensitive to diboson resonances — slightly more than the fully hadronic channel — but much less sensitive to triboson resonances. First, because the would-be reconstructed diboson mass, $m_{\ell\nu J}$, does not peak at the WZX invariant mass for a triboson resonance, but is instead much broader. And, especially, because the event selection implemented by both the ATLAS and CMS Collaborations include a veto on b -tagged jets in order to reduce the background from $t\bar{t}$ production, and this veto suppresses the signals where X has dominant decay into $b\bar{b}$. We restrict ourselves to the ATLAS analysis, as the CMS one follows a similar strategy, and present our results, conveniently normalised as in the previous cases, in figure 8. We consider the WZ selection, that is, a window of ± 13 GeV around the expected Z mass peak for the jet mass m_J .

The two benchmark models with $X \rightarrow q\bar{q}$ seem to be disfavoured by the null result of the ATLAS search [8], as is the benchmark with $W' \rightarrow ZY^\pm \rightarrow WZH$. However, the caveat is that the normalisation of the SM background in this analysis is determined from a fit using two control regions:

- (i) the W control region, with the same event selection as for the signal region but inverting the jet mass requirement: $50 < m_J < 70.2$ or $m_J > 106.4$ GeV;
- (ii) the top control region, with the same event selection as for the signal region but requiring a b -tagged jet instead of vetoing them.

For illustration, we collect in table 3 the efficiency for triboson signals in the W and top control regions, referred to the efficiency for the $WZ + WW$ signal region. The number

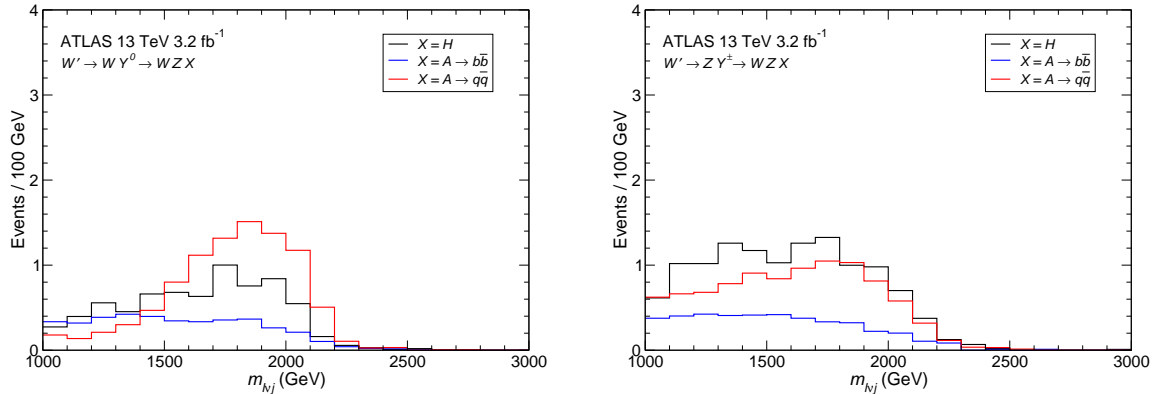


Figure 8: Reconstructed $\ell\nu J$ mass distribution for triboson signals in the ATLAS Run 2 $\ell\nu J$ analysis [8], in the WZ selection.

of data events in the $m_{\ell\nu J}$ distributions for the signal and top control regions is of the same order, and around 5 times larger for the W control region. From this exercise we can conclude that the benchmarks with $X = A \rightarrow q\bar{q}$ indeed seem disfavoured by current measurements, while the rest, especially for $A \rightarrow b\bar{b}$, are compatible with the current limits.

	$X = H$	$X = A \rightarrow b\bar{b}$	$X = A \rightarrow q\bar{q}$
Y^0	1 : 1.20 : 0.55	1 : 0.40 : 0.90	1 : 0.40 : 0.10
Y^\pm	1 : 0.55 : 0.75	1 : 0.35 : 1.60	1 : 0.35 : 0.05

Table 3: Efficiencies ϵ for triboson signals in the W and top control regions, relative to the efficiency in the signal region, using the notation 1 : ϵ_W : ϵ_{top}

4.5 CMS Run 2 search in the $\ell\ell J$ channel

Diboson searches in this final state are performed by looking at a peak in the invariant mass distribution of two oppositely-charged leptons and a boson-tagged jet. Triboson signals do not exhibit a peak in the $\ell\ell J$ invariant mass distribution near the heavy resonance mass $M_R \simeq 2$ TeV, but a peak may appear — if the event selection looking for high-mass resonances does not suppress it — at the Y^0 mass, resulting from the decay $Y^0 \rightarrow ZX$. The CMS Collaboration performs two separate searches in this channel with Run 2 data [13]: one aiming for low-mass resonances with masses 0.55 – 1.4 TeV, and a second one for resonances in the range 0.8 – 2.5 TeV. We will focus here in the low-mass search, and for the high-mass range we will consider the ATLAS search [9]. The CMS

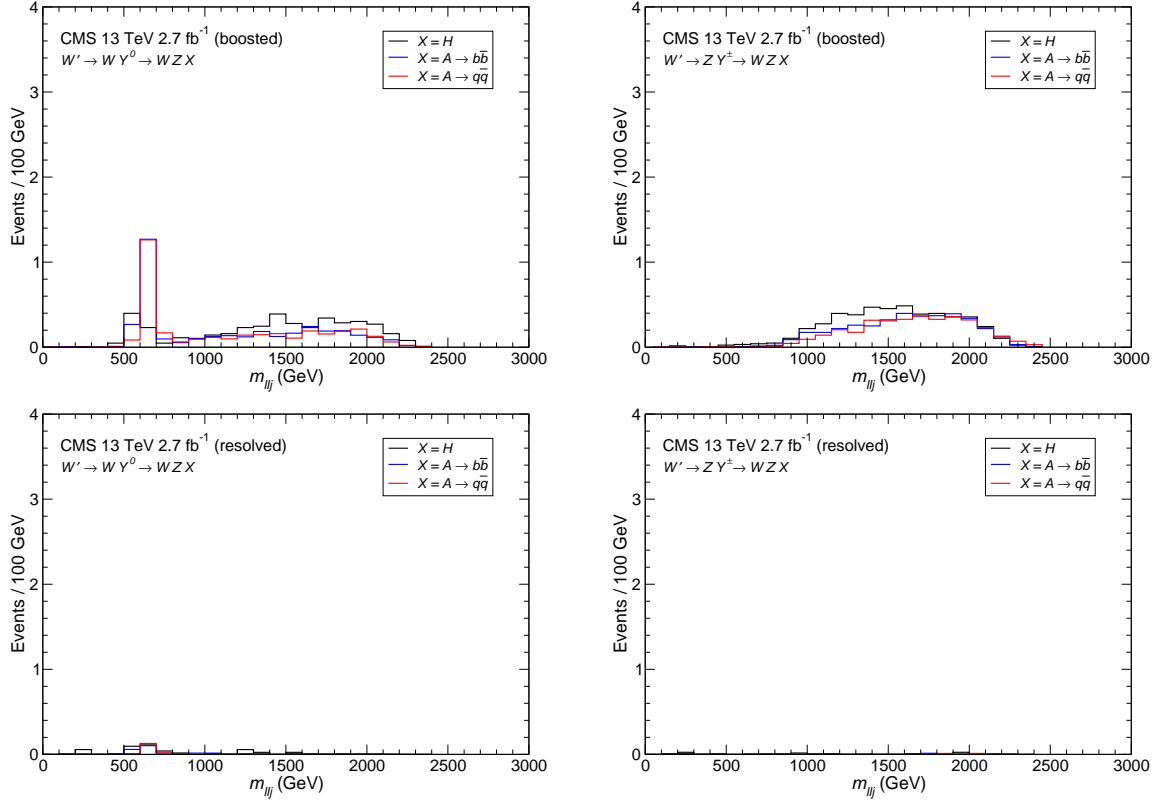


Figure 9: Top: reconstructed $\ell\ell J$ mass distribution for triboson signals in the CMS Run 2 $\ell\ell J$ low-mass boosted analysis [13]. Down: the same, for the low-mass resolved analysis.

low-mass search includes two channels, the boosted channel where a high-purity large- R ($R = 0.8$) fat jet with mass $65 \text{ GeV} < m_J < 105 \text{ GeV}$ is found, in which case it is the candidate for the vector boson V , and the resolved channel where such a jet is not found but instead a pair of small-radius ($R = 0.4$) jets with invariant mass $65 \text{ GeV} < m_{jj} < 110 \text{ GeV}$ exists. In the latter case, V is reconstructed from this jet pair (see appendix A and Ref. [13] for details). The boosted channel is the one where the CMS excess is most prominent. We give our results in figure 9, without separation into b -tagged and untagged samples. Although WZX production alone clearly cannot explain the size of this excess (around 30 events), and additional sources are needed for the production of the ZV resonance, there are several lessons to be drawn:

- (i) The signal is largest in the boosted sample, as it is expected for the decay of a heavy resonance. (We note again that the CMS excess is found mainly in this sample.) The possibility that the CMS excess arises from the decay of a heavy resonance is also in agreement with the fact that no excess was seen in Run 1 analyses.
- (ii) In 57% of the decays of the heavy resonance $R \rightarrow Y^0 W \rightarrow WZX$, the particle X

is more energetic than the W boson. Then, if the fat jets they produce are both V -tagged, the reconstruction algorithm will select the one resulting from X with a slightly larger probability. This makes the $\ell\ell J$ peak near the Y^0 mass prominent over the continuum at higher $m_{\ell\ell J}$, when the selected jet corresponds to the W boson.

If this excess is confirmed, the identity of the particle X and its mass will have to be determined using additional searches in leptonic decay modes.

4.6 ATLAS Run 2 search in the $\ell\ell J$ channel

The ATLAS search for diboson resonances in this final state uses an event selection targeting high masses. Its sensitivity to triboson signals is poor not only because the Z boson leptonic branching ratio is small, but also because the $m_{\ell\ell J}$ distribution does not exhibit a peak at the heavy resonance mass, which would be relatively easy to spot due to the smaller background. In addition, the sensitivity is reduced with respect to diboson resonances by the requirement in the event selection that the dilepton pair and the boson-tagged jet have transverse momenta $p_T^{\ell\ell} > 0.4 m_{\ell\ell J}$, $p_T^J > 0.4 m_{\ell\ell J}$. We present the results of our simulations conveniently normalised in figure 10, for the WZ selection, namely asking that the jet mass lies in a window of ± 15 GeV around the expected W mass peak. As anticipated, the sensitivity is very poor, and the prediction of one event in the full range $1.5 - 2$ TeV is quite compatible with the null result of ATLAS searches in this channel.

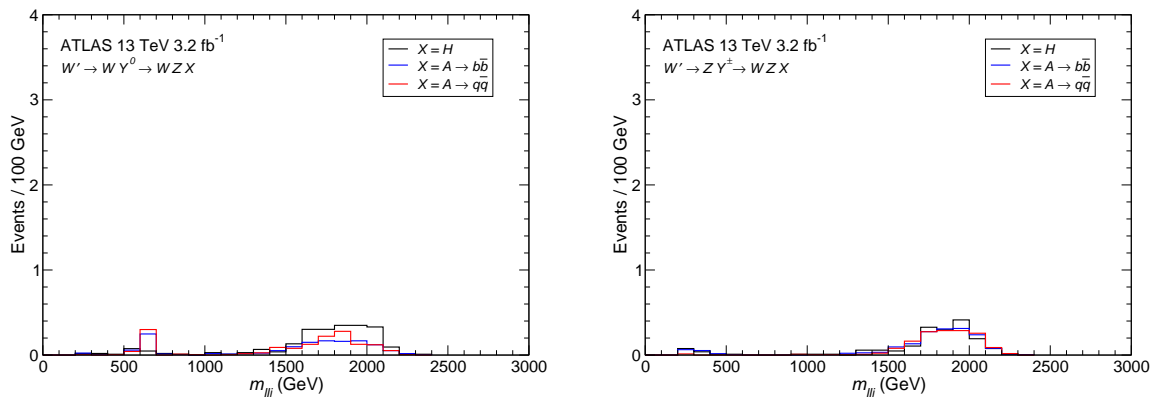


Figure 10: Reconstructed $\ell\ell J$ mass distribution for triboson signals in the ATLAS Run 2 $\ell\ell J$ analysis [9], in the WZ selection.

4.7 ATLAS searches for VH final states

In addition to the searches for a heavy resonance decaying into two gauge bosons, the ATLAS and CMS Collaborations have investigated new heavy resonances decaying into a gauge boson plus a Higgs boson (VH). We use the three analyses in Ref. [27], for final states with 0-leptons, 1-lepton and 2-leptons, to test the sensitivity to triboson signals. The 0-lepton, 1-lepton and 2-lepton VH searches are similar to the above discussed $\nu\nu J$, $\ell\nu J$ and $\ell\ell J$ diboson searches, respectively, with the main difference that for the fat jet an invariant mass window of $75 - 145$ GeV is considered, and b tagging is applied. (In the 1-lepton VH search b tagging is applied instead of the b veto in the $\ell\nu J$ search.) We present the results of our simulations for these analyses, with the previously used normalisation, in figure 11. In all cases the predictions of our benchmark scenarios are compatible with the results of the searches, including the one-lepton channel where a handful of events above the SM prediction are observed in the $1.5 - 2$ TeV range. (In addition, one has to consider again that the signal populates the W and top control regions as for the $\ell\nu J$ channel.) We also note that in the 2-lepton final state, for $Y^0 \rightarrow ZH$ and $Y^0 \rightarrow ZX$, $X \rightarrow b\bar{b}$ a small peak is produced at the Y^0 mass, although the analysis is not optimised for the low-mass region and this peak is invisible in data.

5 Triboson discovery strategies

The identification of a triboson resonance in the current ATLAS and CMS analyses in the fully hadronic channel is not easy, as they search for an excess in the invariant mass distribution of (only) two boson-tagged jets. One strategy that one might consider applying in the ATLAS searches is to remove the p_T asymmetry cut to look for an enhancement at lower dijet invariant masses, as predicted by the simpler analysis performed in Ref. [6]. However, the size of this enhancement is somewhat dependent on the mass of the intermediate particle Y^0/Y^\pm and the details of the jet filtering procedure, and can only be estimated with a more detailed simulation like the one performed here. This is so because, as mentioned before, the kinematical configurations where two of the bosons merge into a single jet may also pass the event selection criteria, due to the jet filtering performed, and these configurations produce two fat jets with similar transverse momentum.

We give in figure 12 the dijet invariant mass distributions with and without the p_T asymmetry cut for the benchmark with $Y^0 \rightarrow ZA$, $A \rightarrow b\bar{b}$, after applying the event selection of the ATLAS Run 1 and Run 2 analyses. We see that the effect of the removal of this requirement is not as pronounced as it was obtained in Ref. [6] with a simpler simulation, especially at Run 1. Moreover, the effect is also mass-dependent, so this test

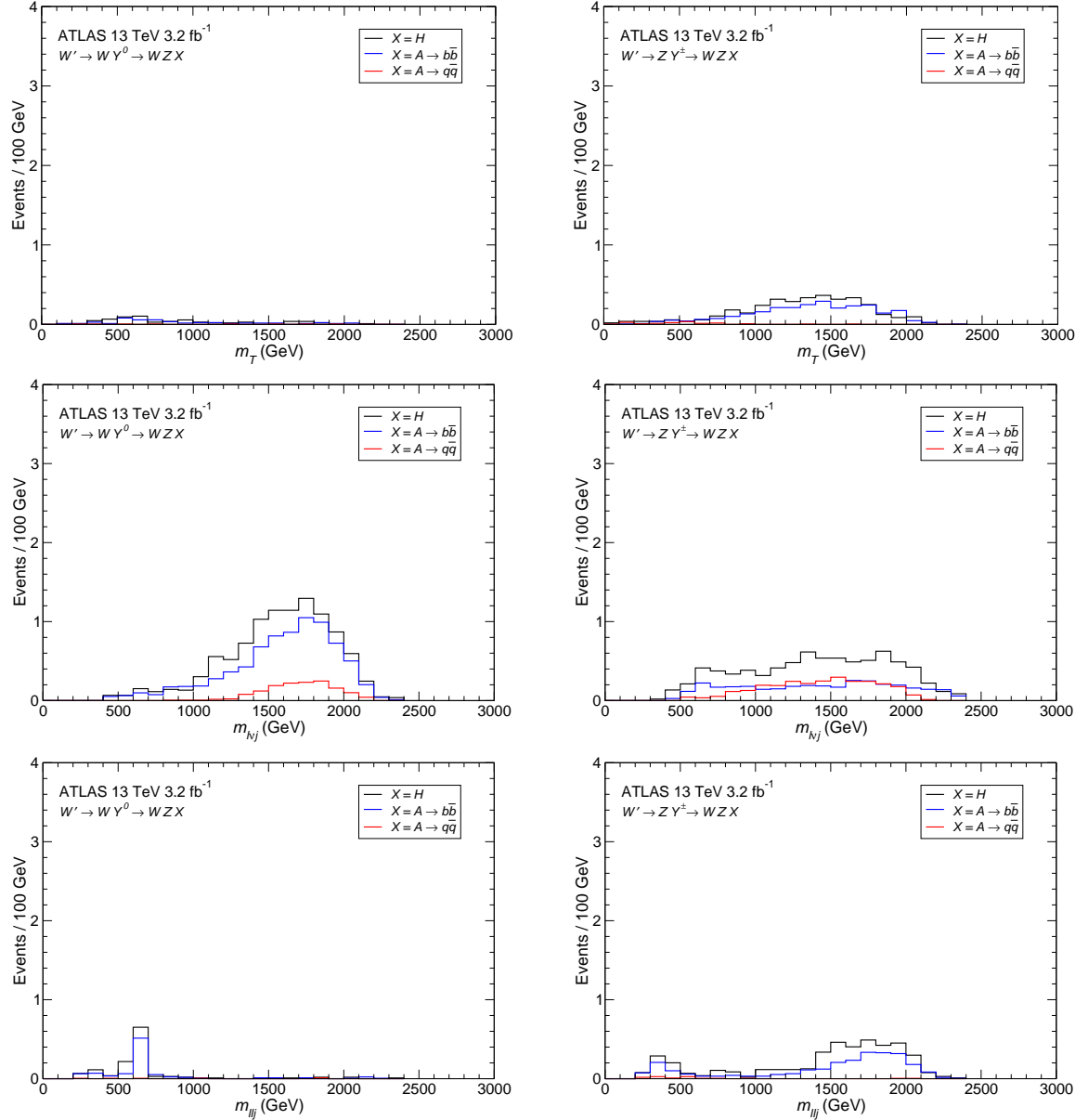


Figure 11: Reconstructed invariant masses for the ATLAS VH analyses [27] Top: transverse mass distribution for the 0-lepton final state. Middle: reconstructed $\ell\nu J$ invariant mass distribution for the 1-lepton final state. Bottom: reconstructed $\ell\ell J$ invariant mass distribution for the 2-lepton final state.

cannot be used to probe the presence of a triboson resonance.

A very simple modification of the ATLAS Run 2 analysis that would enhance the significance of a triboson signal would be to ask in the event selection for the presence of a third softer jet, say with $p_T \geq 50$ GeV, and consider as discriminating variable the three-jet invariant mass, keeping the rest of the event selection criteria, except the N_{trk}

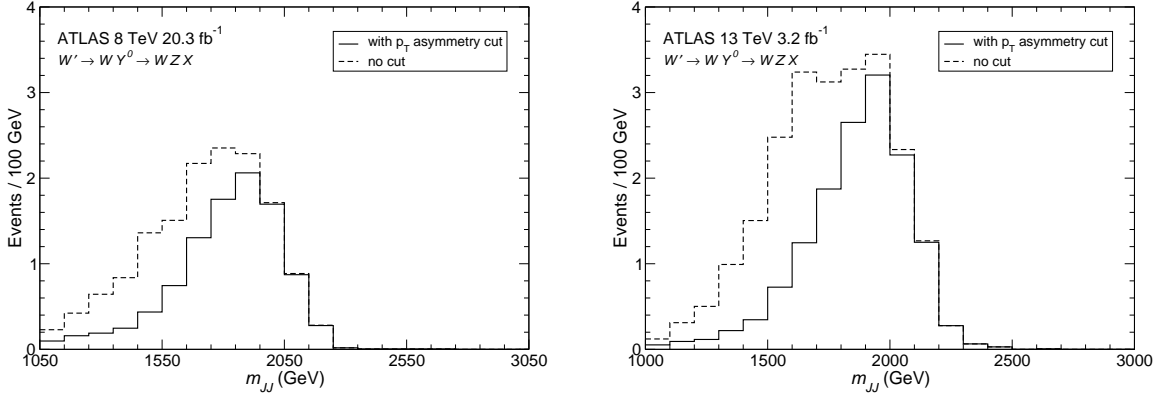


Figure 12: Dijet invariant mass distribution for a selected triboson signal (see the text) in the ATLAS Run 1 (left) and Run 2 (right) fully hadronic analyses, in the WZ selection without N_{trk} , with and without the p_T asymmetry cut.

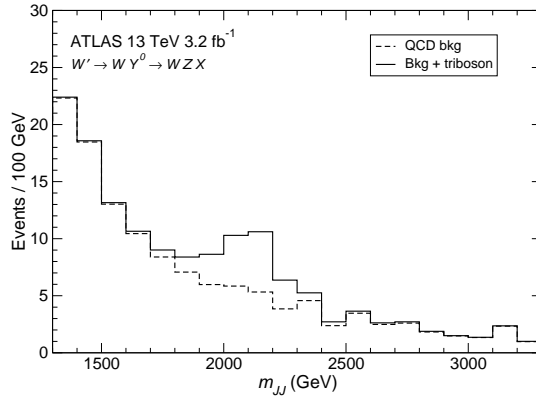


Figure 13: Trijet invariant mass distribution for the SM QCD background and the background plus a triboson signal in the ATLAS Run 2 fully hadronic analysis, in the WZ selection without N_{trk} and without the p_T asymmetry cut.

cut, and optionally removing the p_T asymmetry cut. We show in figure 13 the results of our simulations with such selection, for the case $Y^0 \rightarrow ZA$, $A \rightarrow b\bar{b}$. It is found that 98% of the signal events have such a third jet, therefore the excess is magnified and more localised, with 15 extra events at invariant masses between 1.9 and 2.3 TeV. We have performed pseudo-experiments by taking the numbers of expected events per bin as the mean of a Poisson distribution, and have applied the same likelihood ratio as in section 2 to estimate the signal significance. We find that the expected signal significance is of 4σ for a luminosity of 15 fb^{-1} .

One can also consider dropping one of the cuts on jet masses to enhance the signal.

This is advantageous for lower Y^\pm , Y^0 masses where its decay products often merge into a single jet, but for the benchmark scenarios studied here with $M_R = 2.25$ TeV, $M_{Y^\pm} = M_{Y^0} = 650$ GeV, the increase in the background is much larger than the signal enhancement. Nevertheless, this modification of the analysis strategy might be convenient to study diboson decays of the heavier Z' boson (see section 6).

6 Discussion

In the previous sections we have shown that a triboson signal may explain the excesses observed in the ATLAS Run 1 and Run 2 analyses — observed provided a cut on N_{trk} is not applied in the Run 2 analysis — while still being compatible with a variety of other diboson and VH searches performed. The reason why the application of an upper cut on N_{trk} removes the Run 2 excess, if not a mere statistical effect, remains to be determined. We now turn to the question of the necessary coupling to produce such a signal. As before, we take as reference a signal normalisation of 10 events in the dijet invariant mass interval 1700 – 2100 GeV, and study in detail the case $Y^0 \rightarrow ZX$, with $X = A \rightarrow b\bar{b}$. In this m_{JJ} interval the signal efficiency for this benchmark scenario is of 0.035, relative to all decays of the WZX sample, from which we obtain the necessary cross section

$$\sigma(pp \rightarrow R \rightarrow WZX) = 90 \text{ fb}. \quad (1)$$

For the W' boson of an extended $SU(2)_R$ group with gauge coupling g_R , the production cross section is $\sigma(pp \rightarrow W') \simeq 2.45 g_R^2$ pb at 13 TeV. In a minimal LR extension of the SM, the heavy scalar H_1^0 can play the role of the neutral resonance Y^0 , with a branching ratio $\text{Br}(W' \rightarrow H_1^0 W) \simeq 0.02$ [7]. In this case, the necessary coupling $g_R \simeq 2 g_W$ (being g_W the weak constant) required to reproduce the 2 TeV excess is a bit large, implying in particular a large W' width $\Gamma_{W'} \sim 270$ GeV.¹ Nevertheless, if the quark sector comprises new vector-like singlets — as in grand unified extensions of the SM gauge group — the coupling of the W' boson to SM quarks and correspondingly the decay width into $q\bar{q}'$ are reduced, resulting in a smaller W' width and enhanced branching ratio for $W' \rightarrow H_1^0 W$ [28].

The extension of the SM gauge group with an extra $SU(2)_R$ also contains a new neutral boson Z' . The relation between its mass and the W' mass depends on the particular breaking mechanism of this extra symmetry,

$$M_{Z'} = \frac{k}{\sin \varphi} M_{W'}, \quad (2)$$

¹Searches for $W' \rightarrow t\bar{b}$ do not pose a problem for a large g_R since the partial width for specific states depends on the right-handed quark mixing matrix.

with $k = \sqrt{2}$ (1) if the breaking of $SU(2)_R$ is due to a scalar triplet (doublet), and $\sin \varphi$ a mixing angle determined by the gauge couplings and the SM weak mixing angle by

$$\cos \varphi = \frac{g_L}{g_R} \tan \theta_W \simeq 0.55 \frac{g_L}{g_R} \quad (3)$$

(see for example Ref. [7] for additional details). For the W' mass taken in the benchmark scenarios studied, $M_{W'} = 2.25$ TeV, and the values of g_R that could explain the excess, we would then have $M_{Z'} \simeq 3.2$ TeV if the $SU(2)_R$ breaking is mediated by a triplet. A Z' particle of this mass, and with the couplings to leptons predicted by the LR model, is in conflict with direct searches in the leptonic decay channels; however, these limits would again be relaxed in non-minimal models with a different matter content, or if matter is placed in a different representation of the $SU(2)_R$ group.

As we have mentioned, the lighter particle Y^0 involved in the heavy resonance decay can be the same particle involved in the CMS excess at 650 GeV [13], if for example it decays into ZA , with $A \rightarrow b\bar{b}$. (The possibility that the X particle is the Z boson is disfavoured by the results of the $\ell\nu J$ search, since the main decay channel of the Z boson is into light quarks, and also by the absence of multileptonic signals, but a detailed analysis is necessary to draw any conclusion.) Although in section 4.5 we have seen that the number of events predicted from the decay of the 2.25 TeV resonance is far too small to account for it, other sources of Y^0 particles (i.e. additional decay modes of the 2.25 TeV resonance as well as of heavier ones) may also contribute, since the search is inclusive. In this regard, it is worthwhile pointing out that the Z' decays into SM and heavier bosons² would also be visible in the hadronic diboson searches provided a different analysis strategy is adopted, removing for example one of the cuts on jet masses.

To conclude, in this paper we have shown via detailed simulations the capability for the triboson scenarios to explain a few excesses found in hadronic diboson searches while remaining consistent with null results in other channels. In order to determine whether such excesses indeed correspond to new physics and to discover their physical origin, it is desirable for experiments to consider triboson search strategies in addition to traditional diboson benchmarks. We have investigated a simple modification of the ATLAS hadronic search that makes it more sensitive to this type of resonance. The same strategy could be applied for the CMS search as well. In most of the remaining diboson searches the analysis modifications are obvious, having in mind that a triboson resonance yields not only the two bosons searched for, but also an additional particle.

²For example, $Z' \rightarrow W^+W^-$, $Z' \rightarrow ZH$, $Z' \rightarrow ZH_1^0$, $Z' \rightarrow HA^0$, $Z' \rightarrow H_1^0A^0$, $Z' \rightarrow H^+H^-$ in the specific context of a LR model.

Acknowledgements

We thank M. Perelstein and S. Santos for helpful discussions. This work has been supported by MINECO (Spain) project FPA2013-47836-C3-2-P and by Junta de Andalucía project FQM 101. JC and SL are supported in part by the NSF through grant PHY-1316222.

A Recast of existing diboson searches

Here we provide further details on the recasts of the diboson searches performed in this paper, which include Run 1 and Run 2 hadronic diboson searches from both the ATLAS [1, 12] and CMS [2, 11] Collaborations. Additionally, we reproduce the Run 2 searches in the $\nu\nu J$ [10], $l\nu J$ [8], llJ [9, 13], and VH [27] channels. We use different DELPHES detector cards for each search to incorporate the correct charged lepton isolation requirements.

A.1 ATLAS hadronic diboson channels

We will here describe the Run 2 search for brevity, and refer the reader to Refs. [1] for the details of the very similar Run 1 search. For this analysis, ATLAS employs large- R jets (anti- k_T , $R = 1.0$), denoted as J . Large- R jets are trimmed by re-clustering the large- R jet constituents using the anti- k_T algorithm with $R = 0.2$ and dropping any of the sub-jets with p_T less than 5% of the original jet p_T . Boson candidate jets are tagged for two-prong substructure by imposing a cut on the $D_2^{(\beta=1)}$ variable. Events with charged leptons or $E_T^{\text{miss}} > 250$ GeV are vetoed.

Events must contain two jets J with $p_T > 200$ GeV and $|\eta| < 2.0$. Furthermore, it is required that the the leading large- R jet has $p_T > 450$ GeV and the leading and sub-leading large- R jets J_1, J_2 have

- invariant mass $m_{JJ} > 1$ TeV;
- small rapidity separation $|\Delta y_{12}| < 1.2$;
- transverse momentum asymmetry $\frac{p_{T1} - p_{T2}}{p_{T1} + p_{T2}} < 0.15$.

The jets are tagged as W or Z candidates if their mass is within an interval of ± 15 GeV around the expected resonance peak. Notice that a jet can be simultaneously tagged as W and Z .

A.2 CMS hadronic diboson channel

The Run 2 CMS hadronic search uses large- R anti- k_T jets with $R = 0.8$ (AK8 jets) for hadronic vector boson candidates. Events containing an isolated charged lepton are rejected. Charged lepton isolation requirements are based on reconstructed tracks and calorimeter deposits within $\Delta R = 0.3$. A jet-pruning algorithm is performed on the AK8 jets, which starts from all original constituents of the jet and discards soft recombinations after each step of the Cambridge-Aachen algorithm. Only jets with $|\eta| < 2.4$ are considered.

N -subjettiness is used to classify jet substructure, in particular $\tau_{21} = \tau_2/\tau_1$. AK8 jets with $\tau_{21} > 0.75$ are rejected. The high-purity (HP) category of AK8 jets is defined by $\tau_{21} < 0.45$, and the low-purity (LP) category by $0.45 < \tau_{21} < 0.75$. A jet is considered as tagged if it has $\tau_{21} < 0.75$ and mass in the range $65 \text{ GeV} < m_J < 105 \text{ GeV}$, and it has momentum $p_T > 200 \text{ GeV}$. A jet is considered as W -tagged if its mass is in the range $65 - 85 \text{ GeV}$, and Z -tagged if it is in the range $85 - 105 \text{ GeV}$.

For this analysis, a HP sample is defined by the presence of two boson jets being tagged as HP, whereas a LP sample is defined where one of them is of HP and the other one LP. The leading two jets within these categories must have

- rapidity difference $|\Delta y_{12}| \leq 1.3$;
- dijet invariant mass $m_{JJ} \geq 1 \text{ TeV}$.

The CMS Run 1 analysis is similar, with the main differences that (i) the leading and sub-leading AK8 jets are considered and a cut on τ_{21} is imposed to select HP (or LP) samples, in contrast with the Run 2 strategy of considering all V -tagged AK8 jets and selecting the leading and sub-leading one among them; (ii) a single mass window $70 - 100 \text{ GeV}$ is considered and W/Z discrimination is not attempted.

A.3 ATLAS $\nu\nu J$ diboson channel

For this search, we remove the lepton isolation requirements within the DELPHES ATLAS detector card in order to best match the loose track-based isolation criteria used in the analysis. There are two jet definitions used in this analysis: large- R jets (anti- k_T , $R = 1.0$) denoted J and small- R jets (anti- k_T , $R = 0.4$). The leading large- R jet is trimmed as in the ATLAS fully hadronic channel and, after trimming, it is required to have $p_T > 200 \text{ GeV}$ and $|\eta| < 2$. The missing energy E_T^{miss} is calculated from the vectorial sum of charged leptons and small- R jets. The final event selection criteria are

- large $E_T^{\text{miss}} > 250$ GeV;
- E_T^{miss} isolation: the minimum azimuthal separation between the E_T^{miss} vector and any small- R jet is required to be greater than 0.6 radians;
- events with charged leptons are vetoed;
- the leading large- R jet mass must be consistent with the W or Z boson mass within a window of ± 15 GeV;
- the leading large- R jet must have a two-prong structure (achieved by a cut on the $D_2^{(\beta=1)}$ variable).

Finally, the transverse mass variable is calculated as

$$m_T = \sqrt{(E_{T,J} + E_T^{\text{miss}})^2 - (\vec{p}_{T,J})^2 + (\vec{E}_T^{\text{miss}})^2}, \quad (4)$$

where $E_{T,J} = \sqrt{m_J^2 + p_{T,J}^2}$.

A.4 ATLAS $\ell\nu J$ diboson channel

This search again employs the large- R and small- R jet definitions as above. Small- R jets are used for b -tagging, and events with b -tagged jets are rejected. Leptons must be isolated from tracks with $p_T > 1$ GeV and calorimeter activity within $\Delta R = 0.2$ of the lepton. The main selection criteria include

- large $E_T^{\text{miss}} > 100$ GeV;
- transverse momenta $p_T > 250$ GeV for the leading jet and $p_T > 200$ GeV for the $\ell\nu$ pair; also for both also $p_T > 0.4 m_{\ell\nu J}$ is required, with $m_{\ell\nu J}$ the $\ell\nu J$ reconstructed mass;
- the leading large- R jet mass has to be consistent with the W or Z boson mass within a window of ± 13 GeV;
- the leading large- R jet must have two-prong structure (achieved by a cut on the $D_2^{(\beta=1)}$ variable).

The $\ell\nu j$ reconstructed mass $m_{\ell\nu J}$ introduced above is computed imposing that the $\ell\nu$ pair results from a W boson decay, solving a quadratic equation for the neutrino longitudinal momentum and taking the solution with minimum neutrino longitudinal momentum if both real, or the real part if it is complex.

A.5 ATLAS $\ell\ell J$ diboson channel

For this search, we remove the lepton isolation requirements within the DELPHES ATLAS detector card in order to best match the loose isolation criteria used in the analysis. The same large- R jets with $|\eta| < 2.0$ are used as in other ATLAS analyses. The selection criteria are:

- two same-flavour opposite-sign leptons with $p_T > 25$ GeV and $|\eta| < 2.5$ for muons; $|\eta| < 1.37$ or $1.52 < |\eta| < 2.47$ for electrons;
- dilepton invariant mass $66 \text{ GeV} < m_{\mu\mu} < 116 \text{ GeV}$ for muons, and $83 \text{ GeV} < m_{ee} < 99 \text{ GeV}$ for electrons;
- transverse momentum $p_T > 200$ GeV for the leading jet; also for the leading jet and the $\ell\ell$ pair $p_T > 0.4 m_{\ell\ell J}$ is required, with $m_{\ell\ell J}$ the $\ell\ell J$ invariant mass;
- the leading large- R jet mass has to be consistent with the W or Z boson mass within a window of ± 15 GeV;
- the leading large- R jet must have two-prong structure (achieved by a cut on the $D_2^{(\beta=1)}$ variable).

The $\ell\ell J$ invariant mass is simply calculated from the four-momenta of the two charged leptons and the leading fat jet, scaling the lepton momenta so that their invariant mass coincides with the Z mass.

A.6 CMS $\ell\ell J$ diboson channel

In the low-mass analysis two classes of jets are used: $R = 0.8$ jets (AK8 jets) and $R = 0.4$ jets (AK4 jets). The high-purity category of AK8 jets is defined by $\tau_{21} < 0.45$. A jet is considered as tagged if it is in the high purity category, its mass in the range $65 \text{ GeV} < m_J < 105 \text{ GeV}$, and it has momentum $p_T > 200$ GeV. If such a jet is not found, the reconstruction of the hadronically decaying boson is attempted using pairs of AK4 jets with $p_T > 30$ GeV each, and $p_T(jj) > 100$ GeV, with invariant mass $65 \text{ GeV} < m_{jj} < 110 \text{ GeV}$. For the charged leptons, the following selection criteria apply:

- muons with $|\eta| < 2.4$ and electrons with $|\eta| < 1.44$ or $1.57 < |\eta| < 2.1$ are considered; they must have same flavour and opposite sign, with the leading and sub-leading lepton having with $p_T > 40$ GeV and 24 GeV, respectively;
- for electrons, a minimum separation $\Delta R(ee) \geq 0.3$;

- dilepton invariant mass $76 \text{ GeV} < m_{\ell\ell} < 106 \text{ GeV}$.

A.7 ATLAS VH searches

For these searches, three types of jets are employed: large- R jets with $R = 1.0$, small- R jets with $R = 0.4$ and track jets built from inner detector tracks with $R = 0.2$. The three channels require the presence of at least one large- R jet with $p_T > 250 \text{ GeV}$ and $|\eta| < 2.0$. The leading large- R jet is considered as the H candidate, and its mass is required to be $75 \text{ GeV} < m_J < 145 \text{ GeV}$. b tagging is performed by requiring that at least one of its associated track jets is b -tagged.

In the 0-lepton channel it is required that no loose leptons are present. For this and the two-lepton channel we remove the lepton isolation requirements within the DELPHES ATLAS detector card. Additional requirements are imposed:

- missing energy $E_T^{\text{miss}} > 200 \text{ GeV}$;
- E_T^{miss} isolation: the minimum azimuthal separation between the E_T^{miss} vector and the leading large- R jet is required to be greater than $2\pi/3$ radians, and the separation with any small- R jet it is required to be greater than $\pi/9$;
- events where there is a b -tagged track jet not associated to the Higgs candidate are vetoed.

The transverse mass is reconstructed as for the $\nu\nu J$ channel.

In the 1-lepton channel the presence of exactly one charged lepton with $p_T > 25 \text{ GeV}$ is required, plus $E_T^{\text{miss}} > 100 \text{ GeV}$. Events where there is a b -tagged track jet not associated to the Higgs candidate are vetoed. The $\ell\nu H$ mass is reconstructed in an analogous way to the $\ell\nu J$ channel.

Finally, in the 2-lepton channel the presence of two same-flavour opposite-charge is required, both with $p_T > 25 \text{ GeV}$. For this channel we also remove the lepton isolation requirements within the Delphes ATLAS detector card. The invariant mass windows are $70 \text{ GeV} < m_{ee} < 110 \text{ GeV}$ for electrons and $55 \text{ GeV} < m_{\mu\mu} < 125 \text{ GeV}$ for muons.

B WZX signals and N_{trk}

It is conceivable that for a signal consisting of a diboson pair plus extra particles, the different fat jet reconstruction algorithms and boson tagging requirements used by the

ATLAS Collaboration in the analysis of Run 1 and Run 2 data might result in a somewhat different efficiency of the N_{trk} cut. In order to investigate this possibility, we have considered three representative WZX signals, with (a) $M_X = 100$ GeV, $X \rightarrow u\bar{u}$; (b) $M_X = 100$ GeV, $X \rightarrow b\bar{b}$; (c) $M_X = 300$ GeV, $X \rightarrow W^+W^-$. We have divided the phase space of the $R \rightarrow WZX$ decay into 18 regions according to the separation between the three particles W, Z, X and the energy of X . We have considered:

1. $\Delta\phi_{VV} \equiv \Delta\phi(W, Z)$, the (azimuthal) angle in transverse plane between the W and Z momenta in the laboratory frame. We have separated three regions: $\Delta\phi_{VV} > 2.5$; $2.5 > \Delta\phi_{VV} > 1.2$; (C) $\Delta\phi_{VV} < 1.2$, respectively labelled as ‘A’, ‘B’ and ‘C’.
2. $\Delta R_X \equiv \min(\Delta R(X, W), \Delta R(X, Z))$, separating three regions: $\Delta R_X > 1.2$, $1.2 > \Delta R_X > 0.6$; $\Delta R_X < 0.6$, respectively labelled as ‘1’, ‘2’ and ‘3’.
3. The energy of X in the laboratory frame E_X , separating $E_X < 2M_X$ and $E_X > 2M_X$.

Among the 18 possible combinations only 10 are relevant; the rest are either kinematically forbidden or the phase space is extremely small.

We have generated $pp \rightarrow R \rightarrow WZX$ using a flat matrix element for the decay $R \rightarrow WZX$, so as to avoid any bias introduced by the presence of a secondary resonance Y . Samples of 5×10^4 events are generated for each signal and kinematical configuration, for CM energies of 8 and 13 TeV. On the simulated events we have applied all topological cuts and the jet substructure cuts on \sqrt{y} for ATLAS Run 1 analysis and D_2 for ATLAS Run 2 analysis, as well as the jet mass cuts. For events passing these selection criteria, we have evaluated the efficiency $\epsilon_{N_{\text{trk}}}$ of the N_{trk} cut. The results are shown in Tables 4–6.

	A1	A2	A3	B1	B2
$E_X < 2M_X$	0.83 / 0.83	0.70 / 0.75	0.57 / 0.64	* / *	* / *
$E_X > 2M_X$	0.88 / 0.95	0.8 / 0.7	0.7 / 0.8	0.85 / 0.87	0.84 / 0.85

Table 4: Efficiency of the N_{trk} cut for events passing the remaining selection criteria of the ATLAS Run 1 / Run 2 analyses, for WZX with $X \rightarrow u\bar{u}$, in several phase space regions described in the text. The asterisks indicate those space regions where the overall efficiency of the remaining selection criteria is smaller than 3×10^{-4} .

From this exercise it can be observed that $\epsilon_{N_{\text{trk}}}$ is very similar for Run 1 and Run 2 selections in most cases, and we do not find any phase space region where there is a significant efficiency drop in the Run 2 selection compared to Run 1. Notice that for those regions where we quote only one significant digit for $\epsilon_{N_{\text{trk}}}$, the efficiency of the rest of the

	A1	A2	A3	B1	B2
$E_X < 2M_X$	0.84 / 0.86	0.77 / 0.76	0.56 / 0.66	* / *	* / *
$E_X > 2M_X$	0.89 / 0.88	0.7 / 0.8	0.7 / 0.8	0.89 / 0.88	0.87 / 0.89

Table 5: Same as table 4, for WZX with $X \rightarrow b\bar{b}$.

	A1	A2	A3	B1	B2
$E_X < 2M_X$	0.89 / 0.87	0.85 / 0.83	0.8 / 0.7	0.9 / 0.9	0.9 / *
$E_X > 2M_X$	0.90 / 0.89	0.7 / 0.8	0.7 / 0.6	0.84 / 0.82	0.9 / 0.9

Table 6: Same as table 4, for $X \rightarrow W^+W^-$.

selection cuts is rather small, of the order of 10^{-3} , leading to an uncertainty around ± 0.1 in our evaluation of $\epsilon_{N_{\text{trk}}}$.

References

- [1] G. Aad *et al.* [ATLAS Collaboration], JHEP **1512** (2015) 055 [arXiv:1506.00962 [hep-ex]].
- [2] V. Khachatryan *et al.* [CMS Collaboration], JHEP **1408** (2014) 173 [arXiv:1405.1994 [hep-ex]].
- [3] G. Aad *et al.* [ATLAS Collaboration], Eur. Phys. J. C **75** (2015) 5, 209 [arXiv:1503.04677 [hep-ex]].
- [4] G. Aad *et al.* [ATLAS Collaboration], Eur. Phys. J. C **75** (2015) 2, 69 [arXiv:1409.6190 [hep-ex]].
- [5] V. Khachatryan *et al.* [CMS Collaboration], JHEP **1408** (2014) 174 [arXiv:1405.3447 [hep-ex]].
- [6] J. A. Aguilar-Saavedra, JHEP **1510** (2015) 099 [arXiv:1506.06739 [hep-ph]].
- [7] J. A. Aguilar-Saavedra and F. R. Joaquim, JHEP **1601** (2016) 183 [arXiv:1512.00396 [hep-ph]].
- [8] ATLAS collaboration, note ATLAS-CONF-2015-075.
- [9] ATLAS collaboration, note ATLAS-CONF-2015-071.

- [10] ATLAS collaboration, note ATLAS-CONF-2015-068.
- [11] CMS Collaboration, note CMS-PAS-EXO-15-002.
- [12] ATLAS collaboration, note ATLAS-CONF-2015-073.
- [13] CMS Collaboration, note CMS-PAS-B2G-16-010.
- [14] Y. L. Dokshitzer, G. D. Leder, S. Moretti and B. R. Webber, JHEP **9708** (1997) 001 [hep-ph/9707323].
- [15] M. Cacciari, G. P. Salam and G. Soyez, JHEP **0804** (2008) 063 [arXiv:0802.1189 [hep-ph]].
- [16] J. M. Butterworth, A. R. Davison, M. Rubin and G. P. Salam, Phys. Rev. Lett. **100** (2008) 242001 [arXiv:0802.2470 [hep-ph]].
- [17] A. J. Larkoski, I. Moult and D. Neill, JHEP **1412** (2014) 009 [arXiv:1409.6298 [hep-ph]].
- [18] Additional results in <https://atlas.web.cern.ch/Atlas/GROUPS/PHYSICS/PAPERS/EXOT-2013-08/#auxstuff> .
- [19] V. Khachatryan *et al.* [CMS Collaboration], Eur. Phys. J. C **74** (2014) 11, 3149 [arXiv:1407.3683 [hep-ex]].
- [20] A. Martin and T. S. Roy, Phys. Rev. D **94** (2016) no.1, 014003 [arXiv:1604.05728 [hep-ph]].
- [21] G. Aad *et al.* [ATLAS Collaboration], Eur. Phys. J. C **74** (2014) no.8, 3023 [arXiv:1405.6583 [hep-ex]].
- [22] J. Alwall, M. Herquet, F. Maltoni, O. Mattelaer and T. Stelzer, JHEP **1106** (2011) 128 [arXiv:1106.0522 [hep-ph]].
- [23] T. Sjostrand, S. Mrenna and P. Z. Skands, Comput. Phys. Commun. **178** (2008) 852 [arXiv:0710.3820 [hep-ph]].
- [24] J. de Favereau *et al.* [DELPHES 3 Collaboration], JHEP **1402** (2014) 057 [arXiv:1307.6346 [hep-ex]].
- [25] M. Cacciari, G. P. Salam and G. Soyez, Eur. Phys. J. C **72** (2012) 1896 [arXiv:1111.6097 [hep-ph]].

- [26] J. A. Aguilar-Saavedra. PROTOS, a PROgram for TOp Simulations.
<http://jagular.web.cern.ch/jagular/protos/>
- [27] M. Aaboud *et al.* [ATLAS Collaboration], arXiv:1607.05621 [hep-ex].
- [28] J. H. Collins and W. H. Ng, JHEP **1601** (2016) 159 [arXiv:1510.08083 [hep-ph]].